# Impedance spectroscopy of water splitting reactions on nanostructured metal-based catalysts

# Impedance spectroscopy of water splitting reactions on nanostructured metal-based catalysts

**G A Niklasson, Z Qiu, I Bayrak Pehlivan and T Edvinsson**

Department of Engineering Sciences, Uppsala University, P.O. Box 534, SE-75121 Uppsala, Sweden

Corresponding author: gunnar.niklasson@angstrom.uu.se

**Abstract**. Hydrogen production by water splitting using nanomaterials as electrocatalysts is a promising route enabling replacement of fossil fuels by renewable energy sources. In particular, the development of inexpensive non-noble metal-based catalysts is necessary in order to replace currently used expensive Pt-based catalysts. We report a detailed impedance spectroscopy study of Ni-Mo and Ni-Fe based electrocatalytic materials deposited onto porous and compact substrates with different conductivities. The results were interpreted by a critical comparison with equivalent circuit models. The reaction resistance displays a strong dependence on potential and a lower substrate dependence. The impedance behaviour can also provide information on the dominating reaction mechanism. An optimized Ni-Fe based catalyst showed very promising properties for applications in water electrolysis.

## 1. Introduction

Hydrogen is a promising alternative to fossil fuels and can also be used as energy storage. In particular, it is useful for storing electricity from intermittent renewable sources, which later can be used to produce heat, or alternatively electricity on-demand via fuel cells [1]. Hydrogen can be produced by electrocatalysis of a hydrogen-containing compound such as water. In order to lower the overpotential (i.e., the excess above the thermodynamic requirement of 1.229 V), highly efficient catalysts for the hydrogen evolution reaction (HER) and oxygen evolution reaction (OER) are needed [2]. Currently used highly effective Pt- and Ir-based electrocatalysts need to be replaced by less expensive and more earth-abundant alternatives and here transition metal alloys, oxides/hydroxides or other transition metal compounds are of prime interest [3,4].

The HER is quite well understood in both acidic and alkaline solutions. In the latter case, it is summarized by the following basic reaction steps [5-7]:

$$M + H_2O + e^- \leftrightarrow M - H + OH^- \quad \text{(Volmer step)} \quad (1)$$

$$M - H + H_2O + e^- \leftrightarrow H_2 + OH^- + M \quad \text{(Heyrovsky step)} \quad (2)$$

$$M - H + M - H \leftrightarrow H_2 + 2M \quad \text{(Tafel step)} \quad (3)$$

Here M represents the usually metallic active sites on the surface of the catalyst. It is realized that hydrogen can be produced either by reaction pathway (1) and (2) or by (1) and (3). The OER is considerably more complicated, both in number of possible reaction paths and number of possible steps involved [8,9].

Information on rate-limiting reaction steps and reaction kinetics can be obtained from analysis of so-called Tafel plots depicting the close to exponential dependence of the charge transfer current on overpotential [10], or from frequency-dependent measurements using impedance spectroscopy [6,11]. In the present paper, we focus on the impedance spectroscopy technique and present impedance spectra pertaining to the HER for two transition metal-based electrocatalysts prepared by different methods. The data are interpreted in terms of equivalent circuits, both empirical ones and those that can be derived from the theory of the HER. We especially discuss the substrate dependence of the impedance parameters and discuss the promising properties of a Ni-Fe based catalyst.

## 2. Experimental methods

Ni-Mo films were prepared by reactive DC magnetron co-sputtering using a Balzers UTT 400 unit. The targets were metallic Ni (99.99% purity, Plasmaterials) and Mo (99.99% purity, Plasmaterials) discs. The target to substrate distance was 13 cm. Depositions were done in Ar gas at 30 mTorr pressure, using powers of 80 W and 180 W for Ni and Mo, respectively, onto the following substrates: Ni foam, Ni foil, Carbon cloth (C–cloth), indium tin oxide (ITO) coated glass and fluorine doped tin oxide (FTO) coated glass. The substrate holder was rotated at 3 rpm to improve homogeneity of the films. The film thickness was determined by a Veeco Dektak 150 surface profilometer to 160±10 nm.

Ni-Fe based catalysts were prepared on Ni foam by a hydrothermal method. Ni foam (about 2.5 cm x 3 cm) was reduced in 3 M HCl using an ultrasonic cleaner for 35 min, then washed in deionized water and ethanol for 6 min, and blown dry by nitrogen. Meanwhile, 0.29 g ($Ni(NO_3)_2 \bullet 6H_2O$), 0.4 g $Fe(NO_3)_3 \bullet 9H_2O$ and 0.6 g $CO(NH_2)_2$ were dissolved in 80 ml deionized water under magnetic stirring for 30 min to ensure homogeneity. After dissolution, the aqueous solution was transferred into a 100 ml Teflon-lined stainless steel autoclave. The Ni foam was vertically immersed into the solution with the topside protected by a Kapton tape. Film growth took place for 12 h at 120 $^{o}$C in the autoclave. After cooling down, the sample was ultrasonically washed by deionized water and ethanol in sequence for 6 min to remove residual reactants and then dried at 80 $^{o}$C for 12 h in air.

Electrochemical measurements were carried out in a three-electrode cell at room temperature. The sample was used as working electrode, while Ag/AgCl and a Pt wire or wire mesh were used as reference and counter electrodes, respectively. The electrolyte was 1M NaOH or 1M KOH (pH=14). The measured potential *vs.* Ag/AgCl was converted into the potential scale relative to the reversible hydrogen electrode (RHE) at pH=14. Impedance spectroscopy measurements were performed using a Zahner Zennium electrochemical workstation in the frequency range between 0.7 Hz and 100 kHz. The measurements were done using a 10 mV amplitude AC potential at applied DC potentials between 0 mV and –400 mV *vs.* RHE. Low/high negative values *vs.* RHE are denoted as low/high overpotentials for the HER. Analysis of the impedance data was carried out by the ZView software (Scribner Associates, Inc.).

## 3. Modelling of impedance spectra

A detailed theory for the frequency-dependent impedance of the HER, taking into account all the reaction steps (1)-(3) above, was derived by Harrington and Conway [12]. Their equations can be represented by either of four different equivalent circuits of which the two most used ones are depicted in Figure 1a and 1b. In addition to the elements describing the reaction, these circuits also contain the electrochemical double layer capacitance, $C_{dl}$, and a series resistance $R_s$ due to the substrate and the electrolyte. It is observed that one of the circuits contains an inductance in the reaction part and the other a capacitance. However, if one allows $L_a$ and $C_a$ to take both positive and negative values, the two circuits are equivalent and represent the complete reaction kinetics. Harrington and Conway recommend the circuit in Figure 1a, since it allows a clear physical interpretation. In this case, the resistance $R_{ct}$ is the reaction charge transfer resistance, while the $L_a$-$R_{a1}$ series combination represents the additional part of the impedance response that is due to a changing surface coverage of adsorbed species [12]. Diard et al. performed a detailed analysis of the Volmer-Heyrovsky and Volmer-Tafel reaction sequences [13] and showed that the Volmer-Tafel case always leads to capacitive behaviour,

while the Volmer-Heyrovsky case can exhibit either inductive or capacitive behaviour. It should be noted that these circuits represent ideal reaction kinetics and that in real cases it is often necessary to replace the capacitive elements by constant phase elements (CPE's).

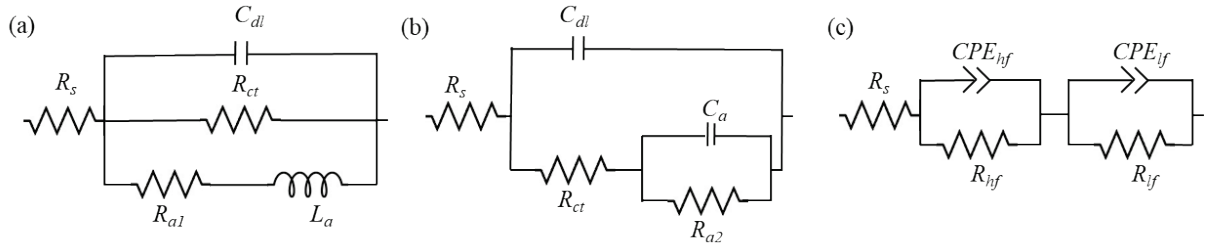


**Figure 1.** Equivalent circuits describing the (a) inductive behaviour and (b) capacitive behaviour predicted for the HER. (c) An empirical equivalent circuit often used to describe the impedance response of the HER.

Figure 1c depicts an empirical circuit that is frequently used to model water splitting reactions. It consists of the series resistance and two *R-CPE* parallel combinations denoted *hf* (high frequency) and *lf* (low frequency). Since ideal capacitive behaviour is seldom seen in impedance spectra, as noted above, we need CPE's instead of capacitances. The CPE behaviour [14] is believed to be related to sample inhomogeneities such as roughness and porosity of the electrodes. The circuit in figure 1c can be motivated by different arguments. Firstly, if the CPE's are replaced by ideal capacitances, it becomes equivalent to the circuit in Figure 1b. These two circuits will still give very similar results when we use CPE's instead of capacitances in both cases. Hence figure 1c may be an alternative way to represent the impedance of the HER. Secondly, in certain cases, the adsorptive part of the impedance related to surface coverage may be neglected in comparison with the charge transfer resistance. In this case the first *R-CPE* parallel combination in fig. 1c is taken to be due to the properties of a resistive interlayer on the electrode, while the second *R-CPE* combination gives $CPE_{dl}$ and $R_{ct}$. It should be noted that a resistive interlayer is to be expected for the materials of interest in this paper. The transition metal based electrodes will oxidize in ambient air, immersion in an alkaline electrolyte will lead to growth of oxide/hydroxide compounds on the surface, and in addition, resistive barriers may occur at the interface with the substrate.

## 4. Results

In this section, we present preliminary results from an impedance spectroscopy study of Ni-Mo and Ni-Fe based catalysts and discuss some implications of the results. We first consider substrate effects on the impedance response of Ni-Mo and then discuss some aspects of a Ni-Fe catalyst showing very promising properties for water splitting.

### *4.1. Substrate effects for a Ni-Mo based catalyst*

Ni-Mo was deposited onto different substrates with sheet resistances ranging from about 0.1 Ω for Ni foam to 43 Ω for ITO. Figure 2 shows experimental data in the complex impedance plane for a Ni-Mo based catalyst on (a) Ni foam and (b) ITO. Intermediate results were obtained for the other substrates. The data in figure 2a shows a well-developed semicircular arc and is typical of low resistance substrates. However, it was found that the data could not be accurately fitted by a single parallel R-CPE combination and instead the circuit in figure 1c had to be used. In figure 2b two distinct semicircular arcs are visible, and it is obvious that the circuit in figure 1c is again valid here. However, experimental data for all substrate cases could also be fitted with the circuit in figure 1b, by replacing the capacitances with CPE's. In order to distinguish these circuit models, we have to study the potential dependence of the fitting parameters.

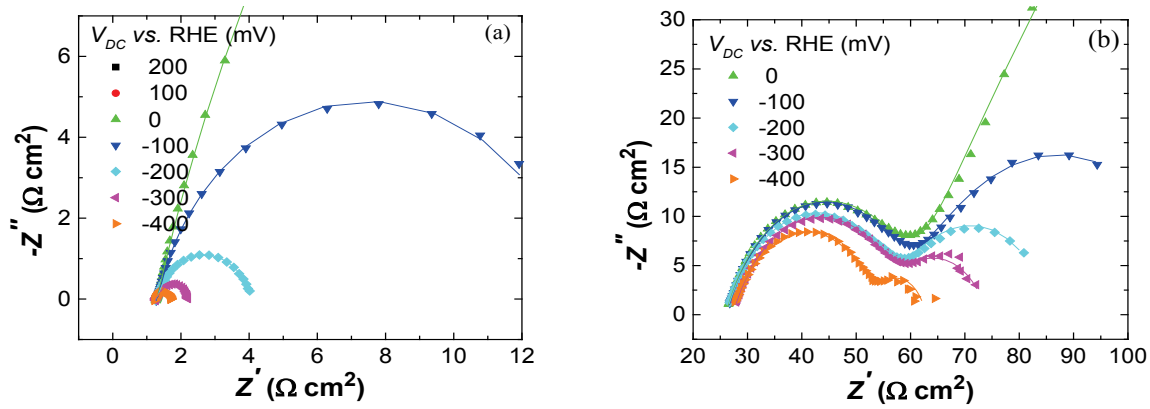


**Figure 2.** Imaginary *vs.* real impedance for a Ni-Mo based catalyst on (a) Ni foam and (b) ITO substrates, for different overpotentials *vs.* RHE. Experimental data are displayed by symbols and fits to the circuit of figure 1c are shown as lines.

The series resistance $R_s$ was not significantly dependent on potential but showed a clear dependence on the sheet resistance of the substrate. It probably has contributions also from the electrolyte since it is slightly above 1 Ω for even the most conducting substrates. The CPE's display a more erratic behavior with no systematic dependence on potential. Figure 3 shows the potential dependence of the low (a) and high (b) frequency resistances obtained from fits to the circuit in figure 1c. The high-frequency resistance, $R_{hf}$, displays no systematic dependence on potential, but shows a strong dependence on the substrate resistance, and exhibits values of the order of, or even lower than $R_s$. On the other hand, $R_{lf}$ shows a systematic dependence on potential, which is close to exponential at high negative potentials. Clearly, it must be identified with the reaction charge transfer resistance. However, in the fit to the circuit in figure 1b, it is $R_a$, which exhibits a systematic potential dependence while $R_{ct}$ has values close to $R_{hf}$. Since the charge transfer resistance should depend on potential, the model behind figure 1b cannot describe all features of the experimental data, and we are obliged to choose the circuit in figure 1c for the analysis. Hence, we must identify $R_{lf}$ with the reaction resistance and $CPE_{lf}$ with the double layer CPE. The high-frequency elements cannot be due to the HER and the strong substrate dependence point to a resistive substrate-film interlayer, perhaps in combination with an oxide/hydroxide layer on the surface.

The reaction charge transfer resistance is closely related to the efficiency of the HER. It is seen in

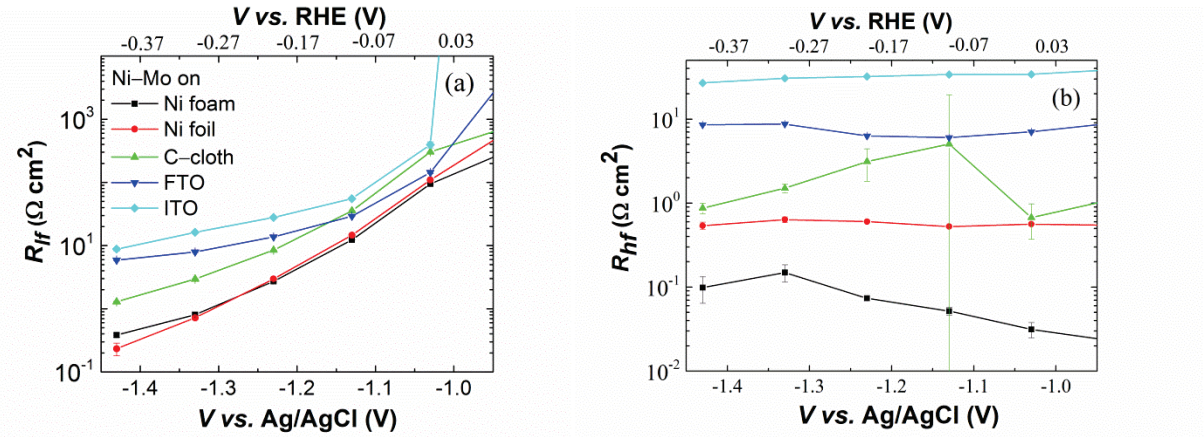


**Figure 3.** Low-frequency resistance (a) and high-frequency resistance (b) obtained from fits of the impedance data in figure 2 to the equivalent circuit in figure 1c. The potential is given both vs. Ag/AgCl (sat) and vs. RHE.

figure 3a that this quantity is lowest for the low resistance substrates, Ni foam and Ni foil, and much higher for the conducting oxide substrates. We conclude that a substrate with low sheet resistance is advantageous for the HER.

*4.2. Impedance response of a Ni-Fe based catalyst*

For this study, we chose Ni foam as the substrate since it gave the best results for the Ni-Mo based catalyst in sect. 4.1. Selected impedance data for the Ni-Fe based catalyst are shown in Figure 4 for two different overpotentials in the HER region. At low overpotentials, figure 4a, an asymmetric semicircular arc is found. On the other hand, at high overpotentials, an inductive behavior is clearly seen at low frequencies, where -Z'' crosses zero. This strongly indicates a Volmer-Heyrovsky mechanism, as discussed above. The crossover between capacitive and inductive behavior is also in qualitative agreement with the theoretical model of the Volmer-Heyrovsky reaction path [13]. The inductive behavior is modelled by the equivalent circuit in figure 1a, resulting in an excellent fit, as seen in figure 4b. However, neither of the theoretical models in figure 1a and 1b give satisfactory fits to the data in figure 4a. Another contribution to the semicircular arc is apparent, and the empirical circuit in figure 1c provides a good fit for the case of low overpotentials. In this case, we assume, as in

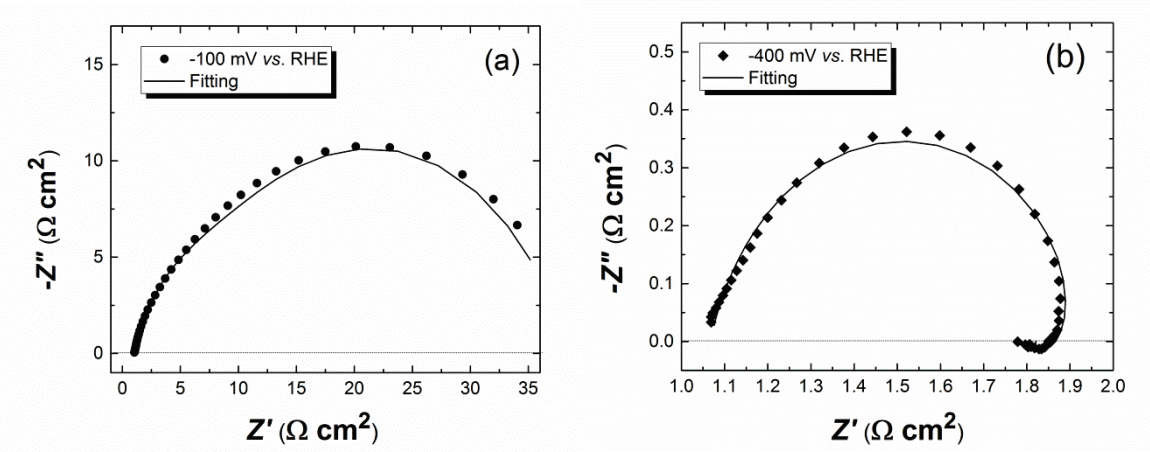


**Figure 4.** Imaginary *vs.* real impedance for a Ni-Fe based catalyst on Ni foam substrate, for two different overpotentials *vs.* RHE. Experimental data are displayed by symbols and fits to the circuit of figure 1c (a) and figure 1a (b) are shown as lines.

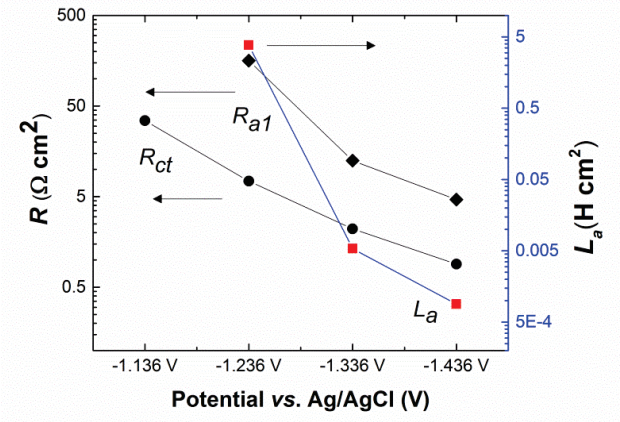


**Figure 5.** Charge transfer resistance $R_{ct,}$ adsorption resistance $R_{a1}$ and inductance $L_a$ are shown as a function of applied potential *vs.* Ag/AgCl (3M KCl). The parameters were obtained from fits of impedance data such as those in figure 4 to the equivalent circuit in figure 1a (circuit 1b was used for -1.136 V).

sec. 4.1, that the high-frequency parameters are due to a resistive interlayer on the substrate or the electrode while the high-frequency resistance is identified with the reaction charge transfer resistance.

We now discuss the potential dependence of the fit parameters. The inductance, $L_a$, as well as the resistance related to the adsorbed species, $R_{a1}$, depend strongly, and in a similar manner, on overpotential, as seen in figure 5. The charge transfer resistance is also potential dependent and exhibits very low values at high overpotentials. On the other hand, the series resistance and the double layer CPE do not significantly depend on potential, as is expected since these quantities depend primarily on the structure of the electrode and the electrochemical cell. The Ni-Fe based catalyst exhibits low reaction resistances both for the HER and the OER and is a very promising material that can be used for the complete water splitting process [15].

## 5. Conclusions

In this paper, we have explored the impedance response of transition metal based catalysts for the hydrogen evolution reaction. By equivalent circuit analysis, we obtain information on parameters describing the reaction kinetics as well as parameters dependent on the structure of the electrode and the electrochemical cell. The reaction kinetics is strongly dependent on the substrate used for the transition metal film, and it was shown that a substrate with low sheet resistance is to be preferred for the HER. In many cases, an impedance response in series with the HER impedance, possibly due to the film-substrate interlayer could be identified. The reaction charge transfer resistance was identified by its characteristic dependence on overpotential.

A Ni-Fe catalyst of prime interest for the OER was shown to display low reaction resistances for the HER as well. The inductive behaviour at high overpotentials indicates that the reaction proceeds according to the Volmer-Heyrovsky scheme. This catalyst is very promising for use on both the anode and cathode side of a water splitting device [15].

## Acknowledgments

We gratefully acknowledge financial support from the Swedish Research Council (VR-2016-03713 and VR-2015-03814) and from the Fuel Cells and Hydrogen 2 Joint Undertaking (Grant No 735218), supported by the European Union (Horizon 2020), Hydrogen Europe and N.ERGHY.

## References

[1] Edwards P P, Kuznetsov V L, Davis W I F and Brandon N P 2008 *Energy Pol.* **36** 4356-4362
[2] Seh Z W, Kibsgaard J, Dickens C F, Chorkendorff I, Nørskov J K and Jaramillo T F *Science* 2017 **335** eead4998/1-eead4998/12
[3] Roger I, Shipman M A and Symes M D 2017 *Nat. Rev. Chem.* **1** 0003/1-0003/10
[4] Shetty S, Sadiq M M J, Bhat D K and Hegde A C 2017 *J. Electroanal. Chem.* **796** 57-65
[5] Bockris J O'M and Potter E C 1952 *J. Electrochem. Soc.* **99** 169-186
[6] Lasia A 2002 Applications of the Electrochemical Impedance Spectroscopy to Hydrogen Adsorption, Evolution and Absorption into Metals *Modern Aspects of Electrochemistry* vol. 35 ed Conway B E and White R E (New York: Kluwer/Plenum) pp. 1-49
[7] Vilekar S A, Fishtik, I and Datta R 2010 *J. Electrochem. Soc.* **157** B1040-B1050
[8] Bockris J O'M 1956 *J. Chem. Phys.* **24** 817-827
[9] Doyle R L and Lyons M E G 2013 *Phys. Chem. Chem. Phys.* **15** 5224-5237
[10] Shinagawa T, Garcia-Esparza A T and Takanabe K 2015 *Sci. Rep.* **5** 13801/1-13801/21
[11] Diard J-P, Landaud P, Le Gorrec B and Montella C M 1988 *J. Electroanal. Chem.* **255** 1-20
[12] Harrington D A and Conway B E 1987 *Electrochim. Acta* **32** 1703-1712
[13] Diard J-P, Le Gorrec B and Maximovitch S 1990 *Electrochim. Acta* **35** 1099-1108
[14] Brug G J, van den Eeden A L G, Sluyters-Rehbach M and Sluyters J H 1984 *J. Electroanal. Chem.* **176** 275-295
[15] Qiu Z, Tai C-W, Niklasson G A and Edvinsson T, to be published.